

Electronic Supplementary Information

Triphenylamine-functionalized tetraphenylpyrazine: facile preparation and multifaceted functionalities

Ming Chen,^a Han Nie,^b Bo Song,^b Lingzhi Li,^a Jing Zhi Sun,^a Anjun Qin^{*ab} and Ben Zhong Tang^{*abc}

^a MOE Key Laboratory of Macromolecular Synthesis and Functionalization, Department of Polymer Science and Engineering, Zhejiang University, Hangzhou 310027, China. E-mail: qinaj@zju.edu.cn or msqinaj@scut.edu.cn (A.J.Q.).

^b Guangdong Innovative Research Team, State Key Laboratory of Luminescent Materials and Devices, South China University of Technology, Guangzhou 510640, China.

^c Department of Chemistry, Institute for Advanced Study, Institute of Molecular Functional Materials, and State Key Laboratory of Molecular Neuroscience, The Hong Kong University of Science & Technology, Clear Water Bay, Kowloon, Hong Kong China. E-mail: tangbenz@ust.hk (B.Z.T.).

Table of contents

Experimental Section	S4
Figure S1. ^1H NMR spectra of 4 in CDCl_3 . The solvent peak is marked with asterisk.	S9
Figure S2. ^{13}C NMR spectra of 4 in CDCl_3 .	S10
Figure S3. ^1H NMR spectra of TPP-Br in CDCl_3 . The solvent peak is marked with asterisk.	S10
Figure S4. ^{13}C NMR spectra of TPP-Br in CDCl_3 .	S11
Figure S5. ^1H NMR spectra of 7 in CDCl_3 . The solvent peak is marked with asterisk.	S11
Figure S6. ^{13}C NMR spectra of 7 in CDCl_3 . The solvent peak are marked with asterisks.	S12
Figure S7. ^1H NMR spectra of TPP-4Br in CDCl_3 . The solvent peak is marked with asterisk.	S12
Figure S8. ^{13}C NMR spectra of TPP-4Br in CDCl_3 .	S13
Figure S9. ^1H NMR spectra of 10 in acetone- d_6 .	S13
Figure S10. ^{13}C NMR spectra of 10 in CDCl_3 . The solvent peak are marked with asterisks.	S14
Figure S11. ^1H NMR spectra of 2 in acetone- d_6 .	S14
Figure S12. ^{13}C NMR spectra of 2 in acetone- d_6 . The solvent peak are marked with asterisks.	S15
Figure S13. ^1H NMR spectra of TPP-TPA in CD_2Cl_2 .	S15
Figure S14. ^{13}C NMR spectra of TPP-TPA in CDCl_3 .	S16
Figure S15. ^1H NMR spectra of TPP-2TPA in CD_2Cl_2 .	S16
Figure S16. ^{13}C NMR spectra of TPP-2TPA in CD_2Cl_2 .	S17
Figure S17. ^1H NMR spectra of TPP-4TPA in CD_2Cl_2 .	S17
Figure S18. HRMS spectra of TPP-TPA.	S18
Figure S19. HRMS spectra of TPP-2TPA.	S18
Figure S20. HRMS spectra of TPP-4TPA.	S19

Figure S21. TGA curves of TPP-TPA, TPP-2TPA and TPP-4TPA measured at a heating rate of 10 °C/min under nitrogen.	S19
Figure S22. Variation in wavelength of TPP-TPA, TPP-2TPA and TPP-4TPA in THF/water mixtures with different water fractions.	S20
Figure S23. PL spectra of TPP-2TPA in THF/water mixtures with different water fractions; $\lambda_{\text{ex}} = 371 \text{ nm}$, $[\text{TPP-2TPA}] = 10^{-5} \text{ M}$.	S20
Figure S24. PL spectra of TPP-4TPA in THF-water mixtures with different water fractions; $\lambda_{\text{ex}} = 387 \text{ nm}$, $[\text{TPP-4TPA}] = 10^{-5} \text{ M}$.	S21
Figure S25. UV-vis spectra (A) and PL spectra (B) of TPP-2TPA in various solvents.	S21
Figure S26. UV-vis spectra (A) and PL spectra (B) of TPP-4TPA in various solvent.	S22
Figure S27. CV curves of TPP-TPA, TPP-2TPA, TPP-4TPA and TPP.	S22
Figure S28. Two-photon PL spectra of TPP-TPA (A), TPP-2TPA (B) and TPP-4TPA (C) with various excitation wavelength in DCM.	S23
Table S1. Optical and thermal properties of TPP derivatives.	S23
Table S2. Theoretical calculation and EC properties of TPA-decorated TPP derivatives and TPP.	S23
References	S24

Experimental Section

Materials: All commercially available chemicals were purchased from J&K, Alfa Aesar, Energy Chemical, or Sinopharm Chemical Reagent Co., Ltd and used directly unless specially stated. 1-(4-bromophenyl)-2-phenylethanone (**3**) was prepared according to the literature procedures.¹ TPP-2Br was provided in our previous work.² THF and toluene were distilled from sodium benzophenone ketyl under dry nitrogen immediately prior to use.

Instrumentation: ¹H and ¹³C NMR spectra were measured with a Bruker AV 400 spectrometer using CDCl₃, CD₂Cl₂, Acetone-*d*₆ or DMSO-*d*₆ as solvent. High resolution mass spectra (HRMS) were carried out using a GCT premier CAB048 mass spectrometer operated in MALDI-TOF mode. Single crystal X-ray diffraction was carried out with a Gemini A Ultra diffractometer at 293K. UV-visible absorption spectra were recorded on a Varian CARY 100 Biospectrophotometer. PL spectra were measured on a RF-5301 PC spectrofluorometer. The absolute quantum efficiency (Φ_F) was recorded on a Hamamatsu Quantaurus-QY C11347 spectrometer. Cyclic voltammetry (CV) was performed in a three-electrode cell using CHI600D electrochemical workstation at room temperature. Electrochemical investigations were conducted in anhydrous CH₂Cl₂ with a Pt disk, Pt wire and SCE as working electrode, auxiliary electrode and reference electrode, respectively. 0.1M *n*-tetrabutylammonium hexafluorophosphate and ferrocene were used as supporting electrolyte and standard, respectively. The electrolyte solution was purged with nitrogen before electrochemical measurements, and the scanning rate was 50 mV s⁻¹. TGA was carried out with TA Q50 at a heating rate of 10°C/ min under N₂, respectively.

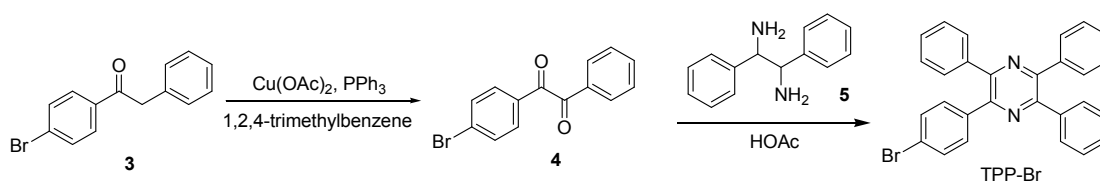
Device fabrication: Electroluminescence device was fabricated on a 80 nm ITO-coated glass with a sheet resistance of 10 Ω/sq. Prior to loading into the pretreatment chamber, the ITO coated glass was soaked in ultrasonic acetone and detergent for one time, followed by two times of ultrasonic de-ionized water and one time of ultrasonic isopropanol. Each time was kept for 10 min. Then, the glass was baked at 80 °C for 1

h in oven, and treated with oxygen plasma for 5 min after dry. Afterwards, ITO-coated glass was transferred to the chamber with a base pressure of 7×10^{-7} Torr for deposition of the organic layers, LiF and Al, with a rate of 1-2 Å/s, 0.1 Å/s and 0.1 Å/s, respectively. The active area of OLED device was 3 mm × 3 mm. The current density-voltage- luminescence characteristics of device were recorded on Keithley 2420 and Konica Minolta chromameter CS-200 analyzers. The EL spectra were recorded with a Photo Research PR-750 spectrofluorometer. All measurements here were carried out under air at room temperature without device encapsulation.

Two-photon excitation fluorescence measurements: The two-photon excitation fluorescence was carried out with a Ti:sapphire femtosecond oscillator (SpectraPhysics Mai Tai) as the excitation source. The output laser pulses have a tunable central wavelength ranged from 690 nm to 1040 nm with pulse duration of less than 100 fs and a repetition rate of 80.5 MHz. The laser beam was focused onto the samples utilizing a lens with a focus length of 3.0 cm. The emission was recorded at an angle of 90° to the direction of the excitation beam to minimize the scattering. The emission signal was directed into a CCD (Princeton Instruments, Pixis 400B) coupled monochromator (IsoPlane160) with an optical fiber. A 700 nm short pass filter was laid before the spectrometer to minimize the scattering from the excitation light. Rhodamine B was selective as reference, and two-photon absorption cross section (σ) could be calculated according to the formula:³

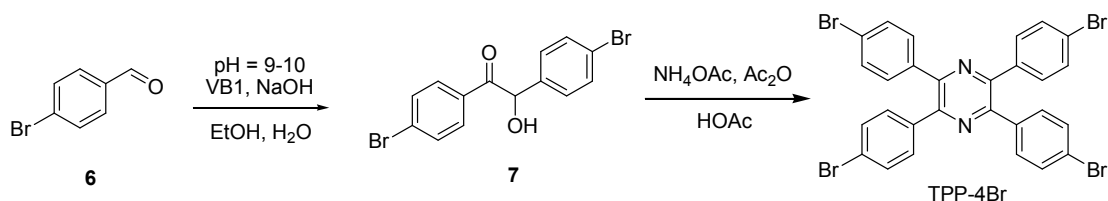
$$\sigma_x = \frac{F_x \phi_0 C_0}{F_0 \phi_x C_x} \sigma_0$$

Where, F , ϕ , and C refer to two-photon fluorescence intensity, fluorescence quantum yield and sample concentration of chromophore, respectively. X and 0 refer to tested sample and reference, respectively.



Synthesis of 1-(4-bromophenyl)-2-phenylethane-1,2-dione (4): The compound was synthesized according to the literature.⁴ Into a 100 mL round bottom flask was added 50 mg (0.273 mmol) of Cu(OAc)₂, 143 mg (0.546 mmol) of PPh₃ and 5 mL of 1,2,4-trimethylbenzene. After stirring for 10 min, 0.5g (1.82 mmol) of **3** dissolved in 2.8 mL of 1,2,4-trimethylbenzene was added into the mixture. The reaction was kept at 100 °C for 2.5 h and then cooled down to room temperature. The mixture was diluted with ethyl acetate (EA), followed by washing by water several time and drying over anhydrous sodium sulfate. The filtrate was concentrated by a totary evaporator and the crude product was purified by a silica-gel column with PE/EA (20:1 by volume) as eluent. Yellow solid was obtained in 49.5% yield. ¹H NMR (400 MHz CDCl₃): δ(TMS, ppm) 7.98 (d, 2H), 7.86 (d, 2H), 7.68 (t, 3H), 7.53 (t, 2H). ¹³C NMR (100 MHz, CDCl₃): δ (TMS, ppm) 193.8, 193.3, 135.1, 132.8, 132.5, 131.7, 131.3, 130.5, 130.0, 129.1.

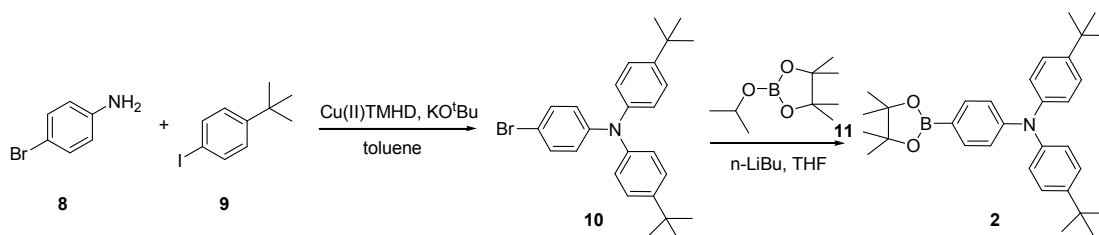
Synthesis of 2-(4-bromophenyl)-3,5,6-triphenylpyrazine (TPP-Br): Into a 50 mL round bottom flask was added 572 mg (2 mmol) of **4**, 420 mg (2 mmol) of 1,2-diphenylethane-1,2-diamine (**5**) and 4 mL of acetic acid. After reflux for 5 h, the mixture was cooled down to room temperature and then filtered. The crude product was purified with recrystallization further in acetic acid. White podwer was obtained in 32.4% yield. ¹H NMR (400 MHz CDCl₃): δ (TMS, ppm) 7.63 (m, 6H), 7.53 (d, 2H), 7.46 (d, 2H), 7.34 (m, 9H). ¹³C NMR (100 MHz, CDCl₃): δ (TMS, ppm) 148.7, 148.5, 148.3, 147.1, 138.3, 138.2, 137.4, 131.5, 131.4, 129.9, 129.8, 128.8, 128.7, 128.4, 128.3, 123.1.



Synthesis of 1,2-bis(4-bromophenyl)-2-hydroxyethanone (7): The compound was synthesized according to the literature.⁵ Into a 250 mL round bottom flask was added 3.75 g (15 mmol) of vitamin B₁, 3.75 mL of water and 75 mL of ethanol. After the mixture was completely dissolved, the system was cooled down below 0 °C with ice

bath, followed by adjusting the pH to 9-10 through adding 10% NaOH aqueous solution. Then, 15 g (81 mmol) of 4-bromobenzaldehyde **6** was added and the reaction was stirred at 65 °C for 18 h. After reaction, the mixture was cooled down to room temperature and filtered, and the filter residue was washed by water and ethanol several times. The filtrate was concentrated and re-dissolved in DCM. The collected organic phase was washed by water several times and dried over anhydrous sodium sulfate. The filtrate was concentrated by a rotary evaporator and the crude product was purified by a silica-gel column with PE/EA (10:3 by volume) as eluent. White solid was obtained in 37.7% yield. ¹H NMR (400 MHz CDCl₃): δ(TMS, ppm) 7.75 (d, 2H), 7.57 (d, 2H), 7.47 (d, 2H), 7.20 (d, 2H), 5.86 (s, 1H). ¹³C NMR (100 MHz, CDCl₃): δ (TMS, ppm) 197.6, 137.6, 132.4, 132.2, 131.9, 130.5, 129.6, 129.4, 123.0, 75.5.

Synthesis of 2,3,5,6-tetrakis(4-bromophenyl)pyrazine (TPP-4Br): Into a 50 mL round bottom flask was added 5 g (13.5 mmol) of **7**, 3.12 g (40.5 mmol) of ammonium acetate, 2 mL (20.25 mmol) of acetic anhydride and 11 mL of acetic acid. After reflux for 3 h, the mixture was cooled down to room temperature, filtered and then washed with hot acetic acid. Pale yellow powder was obtained in 15.2% yield. ¹H NMR (400 MHz CDCl₃): δ (TMS, ppm) 7.49 (s, 16 H). ¹³C NMR (100 MHz, CDCl₃): δ(TMS, ppm) 147.4, 136.6, 131.7, 131.3, 123.7.



Synthesis of 4-bromo-N,N-bis(4-(tert-butyl)phenyl)aniline (10): The compound was synthesized according to the literature.⁶ Into a 50 mL round bottom flask was added 0.66 g (3.84 mmol) of 4-bromoanilines (**8**), 4 g (15.4 mmol) of 4-tert-butyl iodobenzene (**9**), 0.33 g (0.77 mmol) of Cu(II)TMHD and 1.3 g (11.6 mmol) of KO^tBu and 20 mL toluene under nitrogen. After refluxing overnight, the mixture was cooled to room temperature and then concentrated by a rotary evaporator and the crude product was purified by a silica-gel column with PE as eluent. White solid was obtained in 48.2% yield. ¹H NMR (400 MHz CD₃COCD₃): δ(ppm) 7.37 (d, 6H) 7.01

(d, 4H) 6.91 (d, 2H), 1.33 (s, 18H). ^{13}C NMR (100 MHz, CDCl_3): δ (TMS, ppm) 147.3, 146.0, 144.6, 131.9, 126.1, 124.3, 124.0, 113.8, 34.3, 31.4.

Synthesis of 4-(tert-butyl)-N-(4-(tert-butyl)phenyl)-N-(4-(4,4,5,5-tetramethyl-1,3,2-dioxaborolan-2-yl)phenyl)aniline (2): Into a 250 mL round bottom flask was added 0.65 g (1.5 mmol) of **10** and 30 mL of dry THF under nitrogen. The system was cooled down to $-78\text{ }^\circ\text{C}$ and then 0.75 mL (1.8 mmol) of n-BuLi solution was injected slowly. After stirring at $-78\text{ }^\circ\text{C}$ for 1 h, 0.5 mL (1.8 mmol) of 2-isopropoxy-4,4,5,5-tetramethyl-1,3,2-dioxaborolane (**11**) was added, and the reaction was restored to room temperature and stirred overnight. Then, NH_4Cl aqueous solution was added to quench the reaction and the mixture was extracted by DCM. The collected organic phase was concentrated by a rotary evaporator and the crude product was purified by a silica-gel column with PE/DCM (10:1 by volume) as eluent. White solid was obtained in 41.4% yield. ^1H NMR (400 MHz CD_3COCD_3): δ (ppm) 7.57 (d, 2H), 7.38 (d, 4H), 7.03 (d, 4H), 6.91 (d, 2H), 1.31 (d, 30H). ^{13}C NMR (100 MHz, CD_3COCD_3): δ (ppm) 206.2, 151.8, 147.4, 145.6, 136.6, 127.2, 125.8, 121.0, 84.2, 35.0, 31.7, 25.2.

Synthesis of TPP-TPA: Into a 50 mL round bottom flask was added 100 mg (0.22 mmol) of TPP-Br, 77 mg (0.27 mmol) of (4-(diphenylamino)phenyl)boronic acid (**1**), 13 mg (0.011 mmol) of $\text{Pd}(\text{PPh}_3)_4$ and 10 mL of THF under nitrogen. After the mixture was dissolved, 5 mL of 2 M K_2CO_3 aqueous solution was injected. The reaction was kept at $80\text{ }^\circ\text{C}$ for 12 h. Afterwards, the mixture was extracted by DCM, washed by water several times and the organic phase was dried over anhydrous sodium sulfate. The filtrate was concentrated by a rotary evaporator and the crude product was purified by a silica-gel column with PE/DCM (5:1 by volume) as eluent. Pale yellow solid was obtained in 62.7% yield. ^1H NMR (400 MHz CD_2Cl_2): δ (ppm) 7.71 (m, 4H), 7.66 (m, 4H), 7.58 (m, 4H), 7.38 (m, 13H), 7.16 (m, 8H). ^{13}C NMR (100 MHz, CDCl_3): δ (TMS, ppm) 148.4, 148.3, 148.2, 148.0, 147.6, 147.4, 140.7, 138.5, 136.7, 134.2, 130.3, 129.9, 129.3, 128.6, 128.3, 128.2, 127.6, 126.3, 124.5, 123.8, 123.0. HRMS (MALDI-TOF): m/z 627.2666 ($[\text{M}]^+$), calcd for $\text{C}_{46}\text{H}_{33}\text{N}_3$ (627.2674).

Synthesis of TPP-2TPA: The synthetic method was similar to that of TPP-TPA. Kelly solid was obtained in 41.5% yield. ^1H NMR (400 MHz CD_2Cl_2): δ (ppm) 7.69 (m, 9H), 7.56 (m, 8H), 7.38 (m, 7H), 7.29 (m, 8H), 7.12 (m, 14H). ^{13}C NMR (100 MHz, CD_2Cl_2): δ (ppm) 148.8, 148.7, 148.5, 148.4, 148.0, 141.0, 139.1, 137.4, 130.7, 130.2, 129.7, 129.0, 128.7, 128.0, 126.6, 124.9, 124.0, 123.5. HRMS (MALDI-TOF): m/z 870.3695 ($[\text{M}]^+$), calcd for $\text{C}_{64}\text{H}_{46}\text{N}_4$ 870.3722).

Synthesis of TPP-4TPA: The synthetic method was similar to that of TPP-TPA. Kelly solid was obtained in 7.4% yield. ^1H NMR (400 MHz CD_2Cl_2): δ (ppm) 7.76 (d, 8H), 7.59 (m, 16H), 7.30 (d, 16H), 7.05 (m, 24H), 1.32 (s, 72H). HRMS (MALDI-TOF): m/z 1805.0857 ($[\text{M}]^+$), calcd for $\text{C}_{132}\text{H}_{136}\text{N}_6$ 1805.0826).

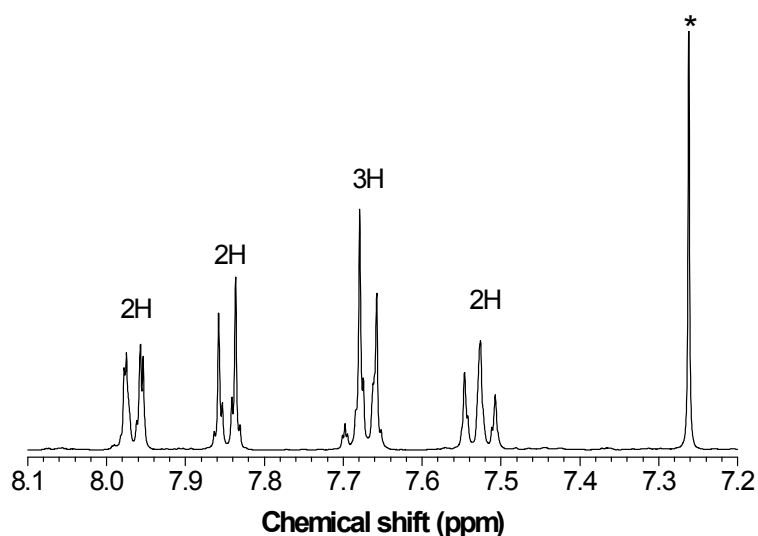


Figure S1. ^1H NMR spectra of **4** in CDCl_3 . The solvent peak is marked with asterisk.

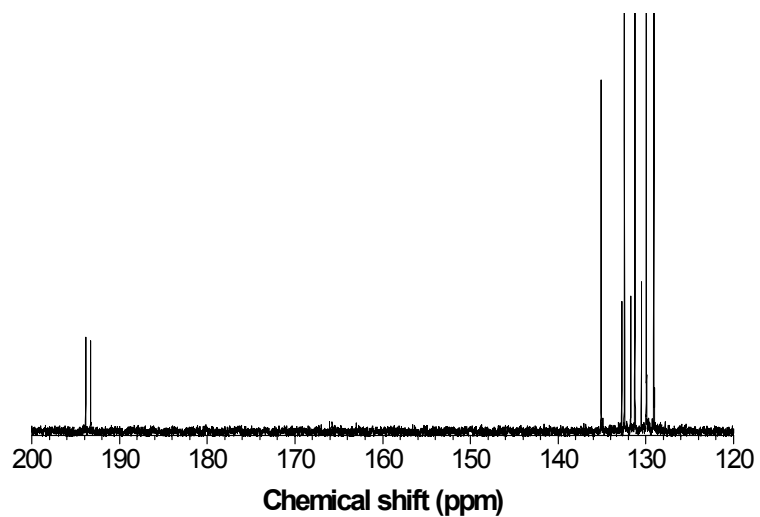


Figure S2. ^{13}C NMR spectra of **4** in CDCl_3 .

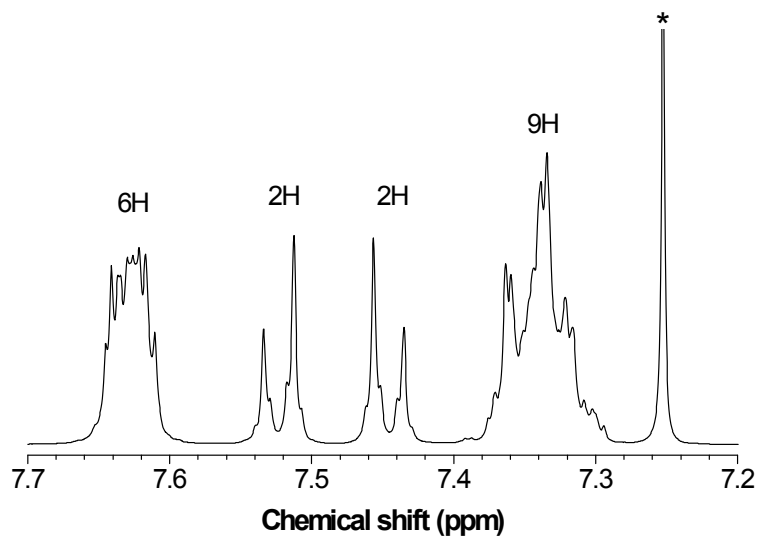


Figure S3. ^1H NMR spectra of TPP-Br in CDCl_3 . The solvent peak is marked with asterisk.

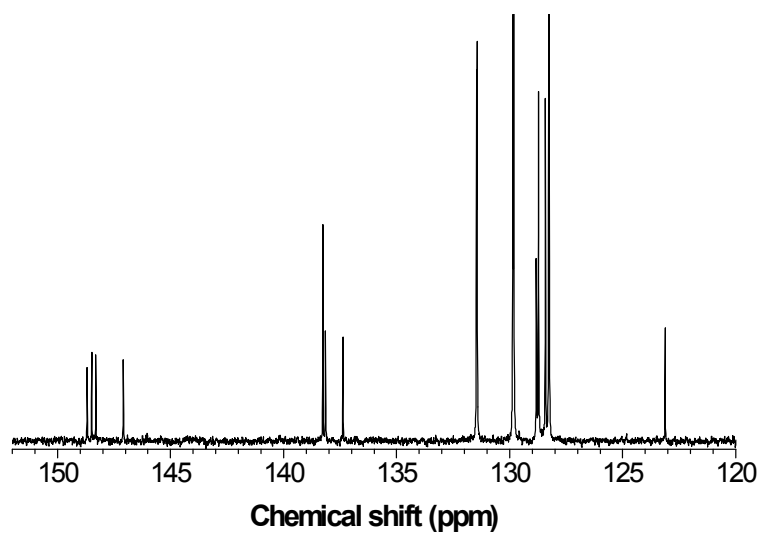


Figure S4. ^{13}C NMR spectra of TPP-Br in CDCl_3 .

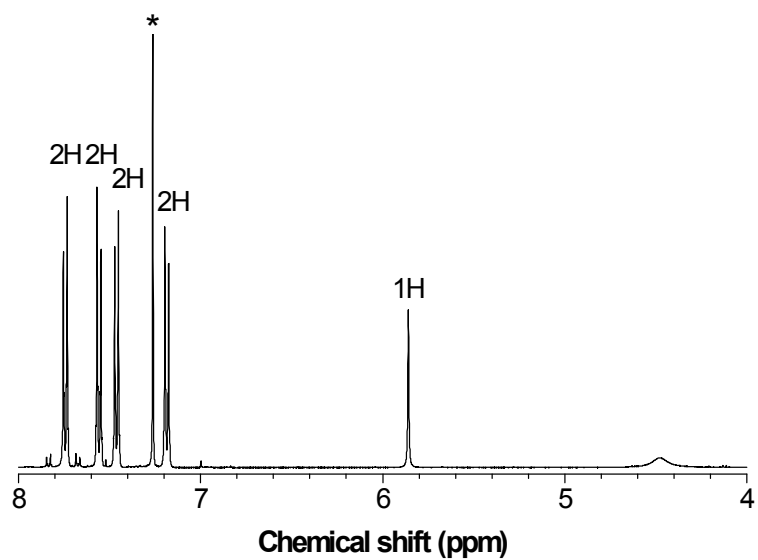


Figure S5. ^1H NMR spectra of **7** in CDCl_3 . The solvent peak is marked with asterisk.

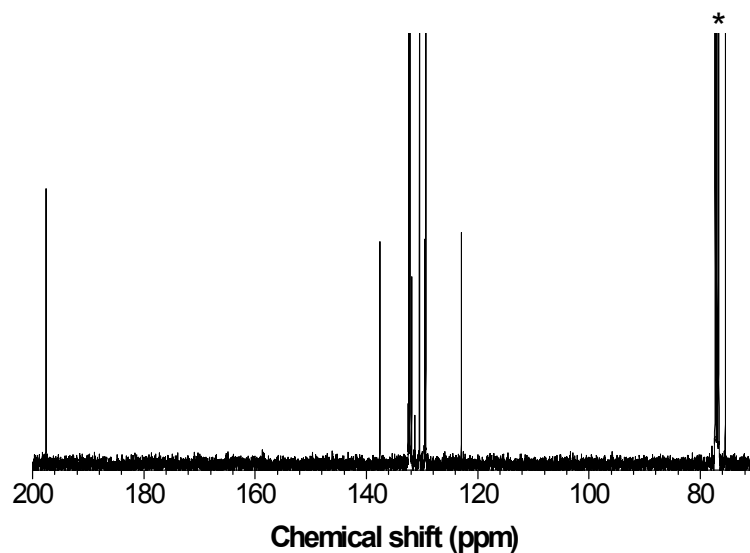


Figure S6. ^{13}C NMR spectra of **7** in CDCl_3 . The solvent peak are marked with asterisks.

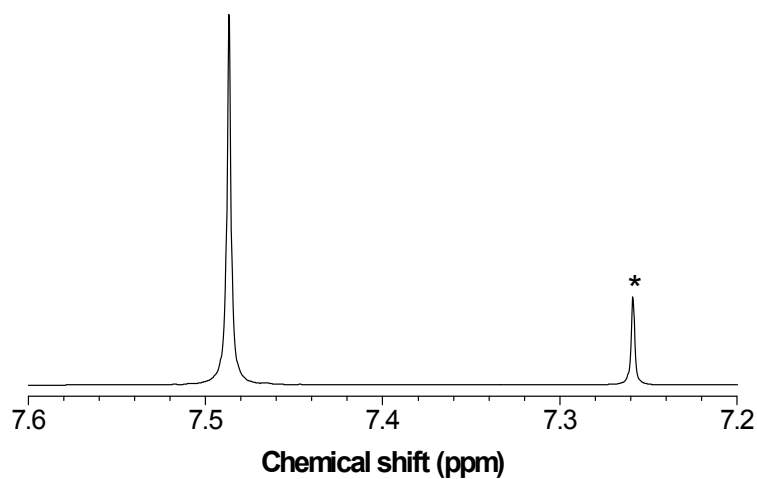


Figure S7. ^1H NMR spectra of TPP-4Br in CDCl_3 . The solvent peak is marked with asterisk.

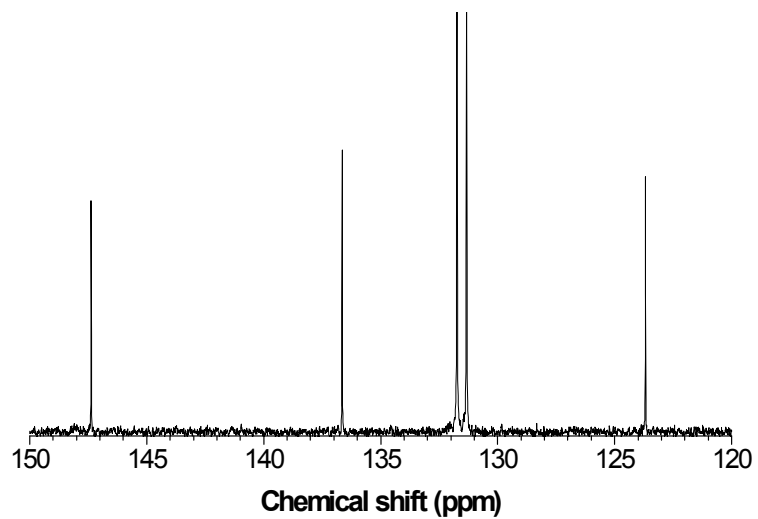


Figure S8. ^{13}C NMR spectra of TPP-4Br in CDCl_3 .

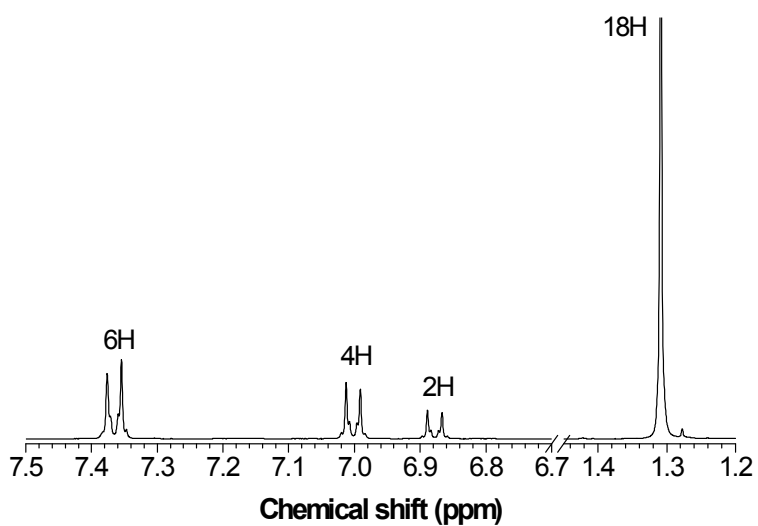


Figure S9. ^1H NMR spectra of **10** in $\text{acetone-}d_6$.

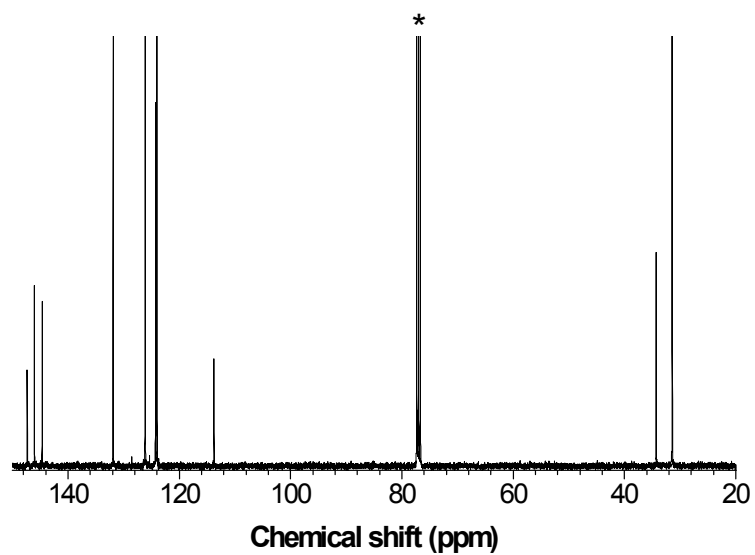


Figure S10. ^{13}C NMR spectra of **10** in CDCl_3 . The solvent peak are marked with asterisks.

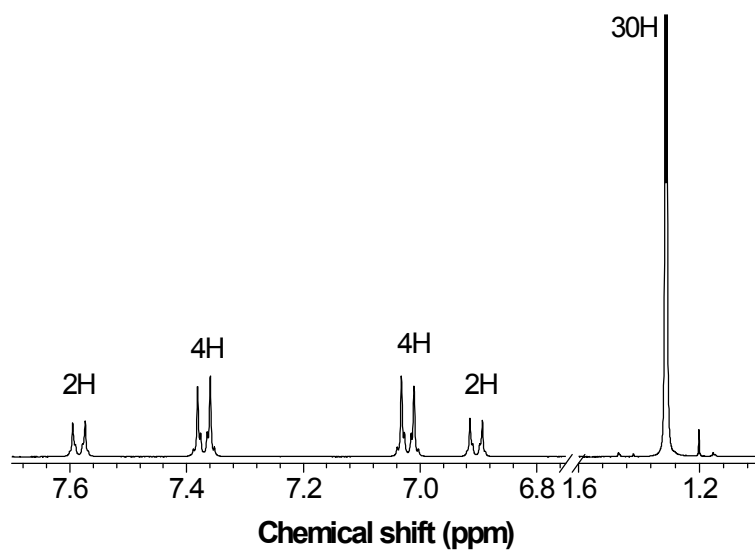


Figure S11. ^1H NMR spectra of **2** in acetone- d_6 .

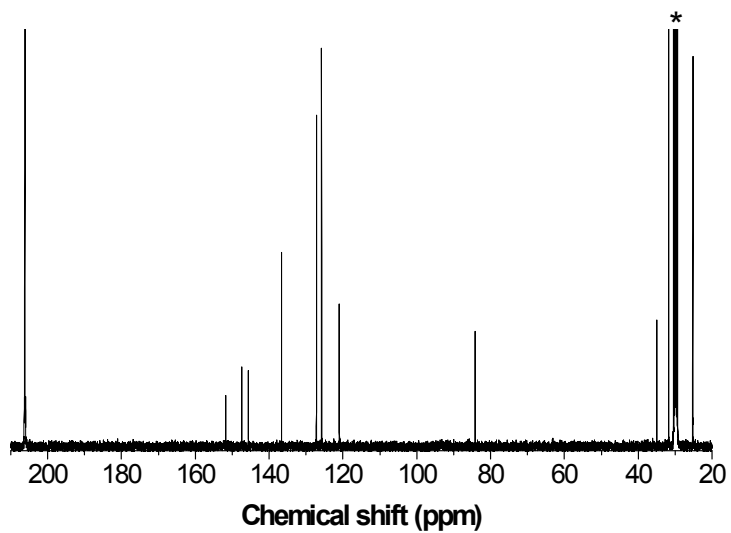


Figure S12. ^{13}C NMR spectra of **2** in acetone- d_6 . The solvent peak are marked with asterisks.

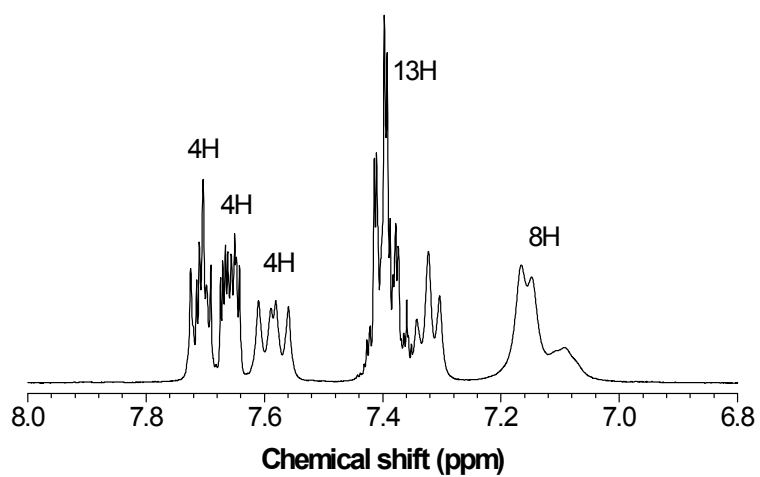


Figure S13. ^1H NMR spectra of TPP-TPA in CD_2Cl_2 .

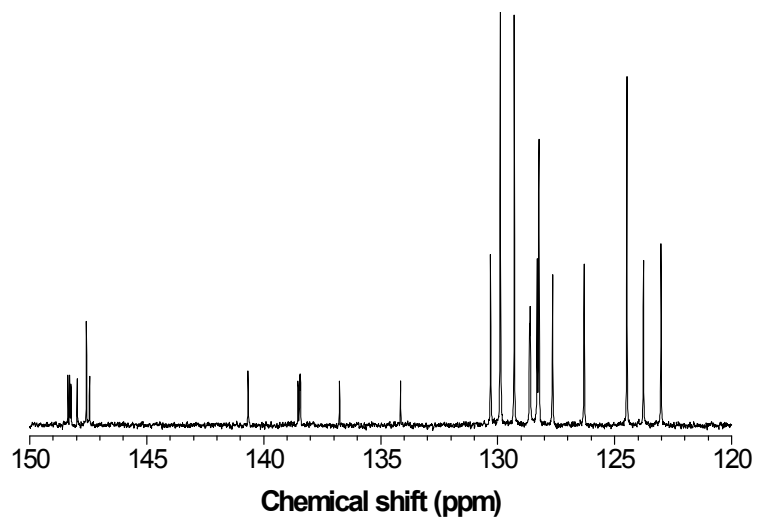


Figure S14. ^{13}C NMR spectra of TPP-TPA in CDCl_3 .

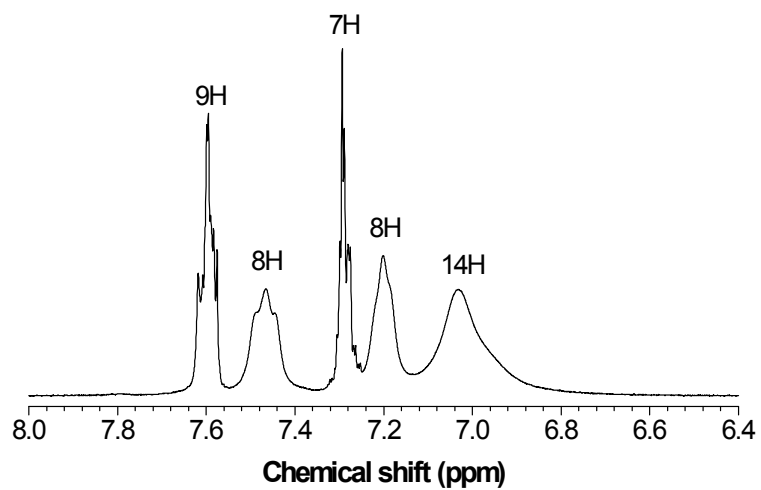


Figure S15. ^1H NMR spectra of TPP-2TPA in CD_2Cl_2 .

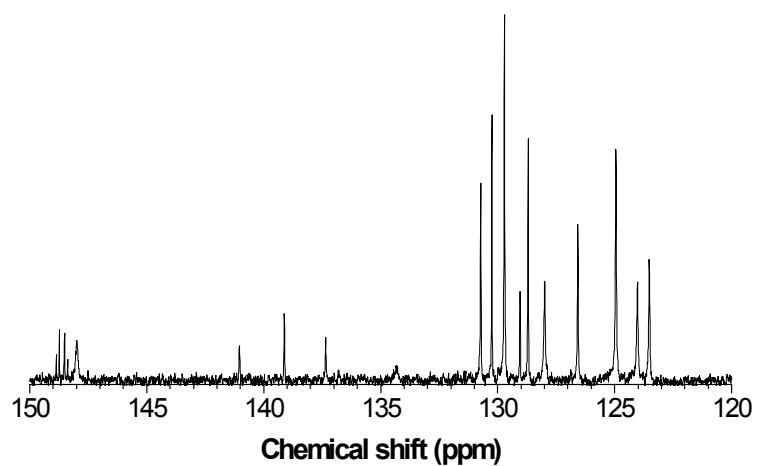


Figure S16. ^{13}C NMR spectra of TPP-2TPA in CD_2Cl_2 .

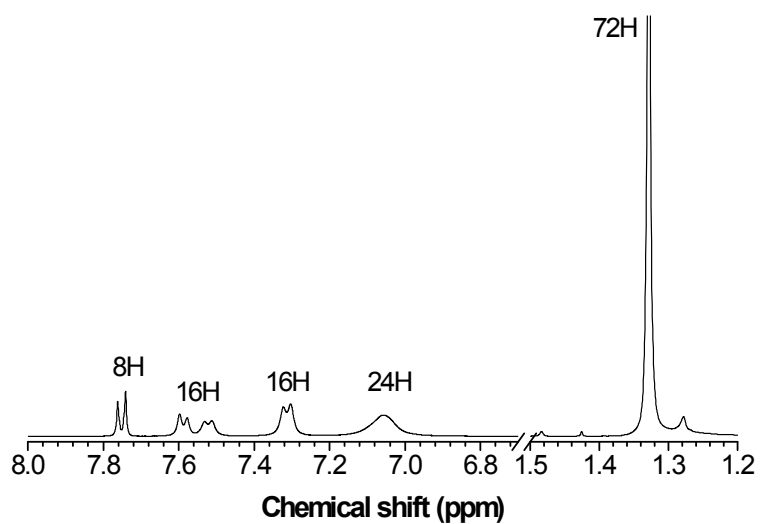


Figure S17. ^1H NMR spectra of TPP-4TPA in CD_2Cl_2 .

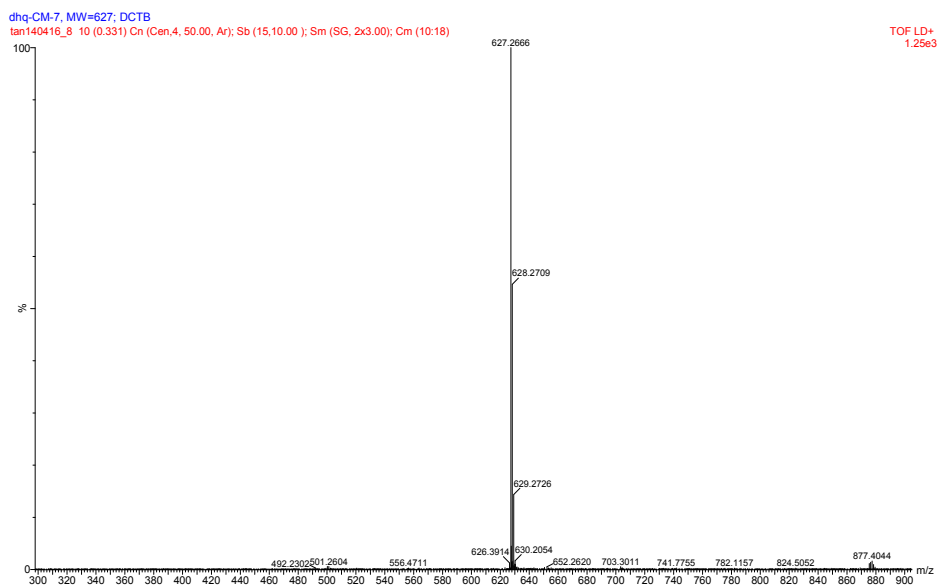


Figure S18. HRMS spectra of TPP-TPA.

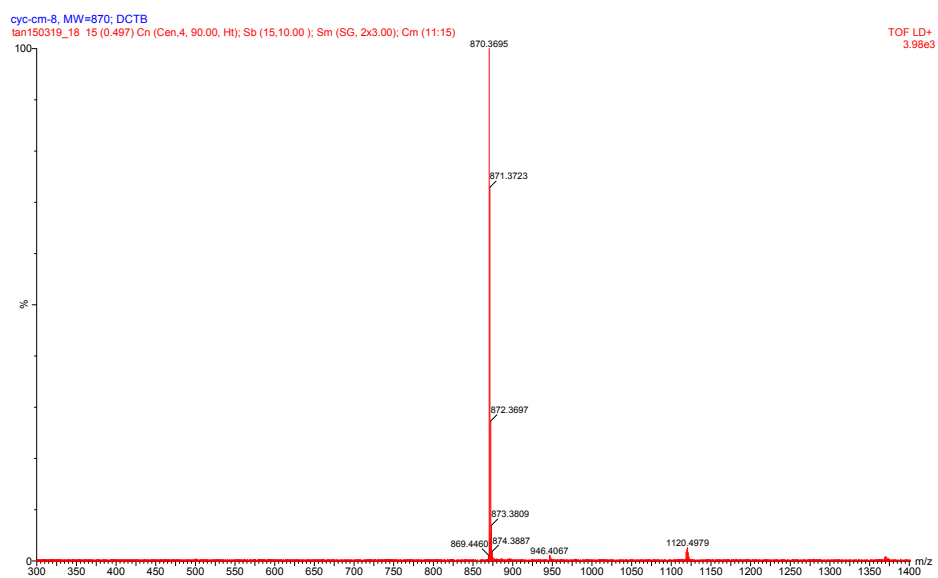


Figure S19. HRMS spectra of TPP-2TPA.

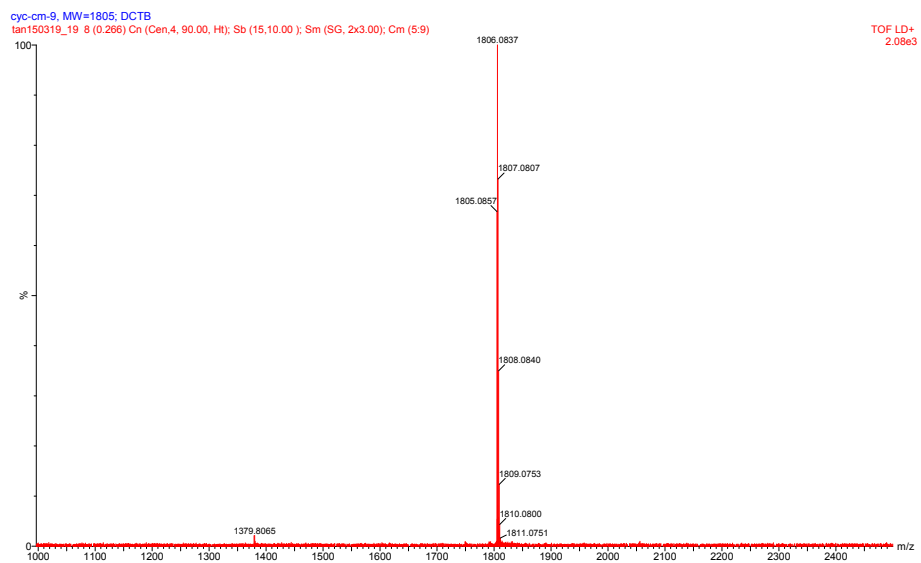


Figure S20. HRMS spectra of TPP-4TPA.

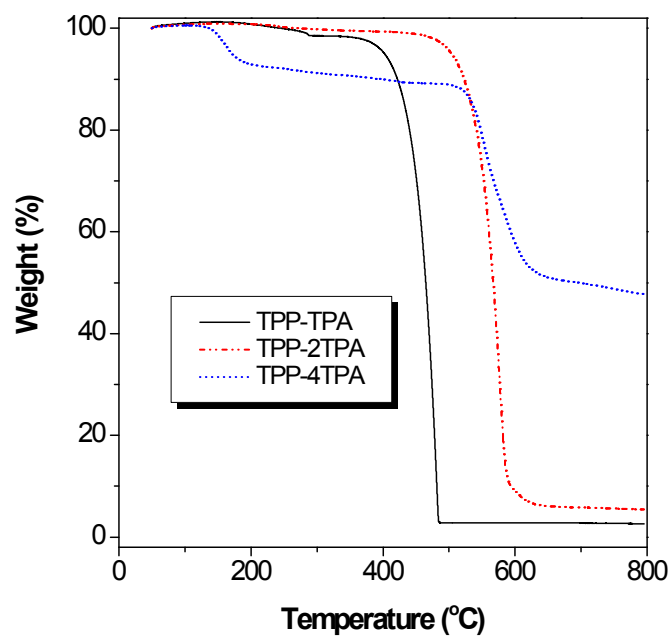


Figure S21. TGA curves of TPP-TPA, TPP-2TPA and TPP-4TPA measured at a heating rate of 10 °C/min under nitrogen.

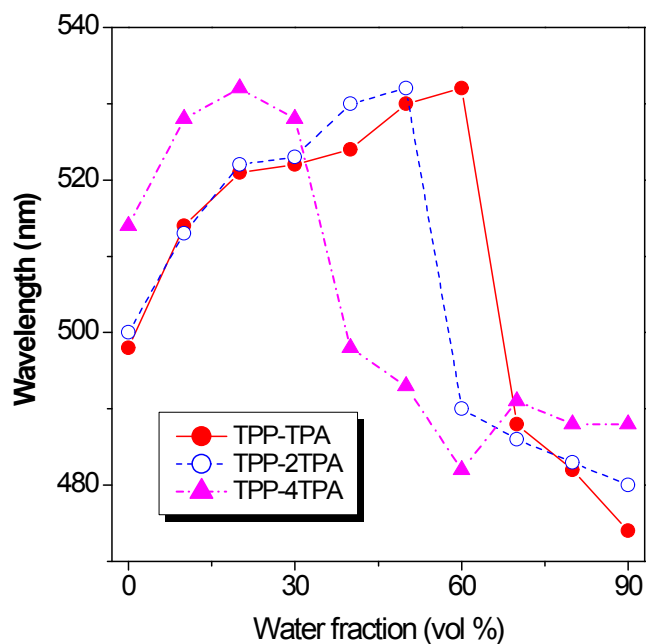


Figure S22. Variation in wavelength of TPP-TPA, TPP-2TPA and TPP-4TPA in THF/water mixtures with different water fractions.

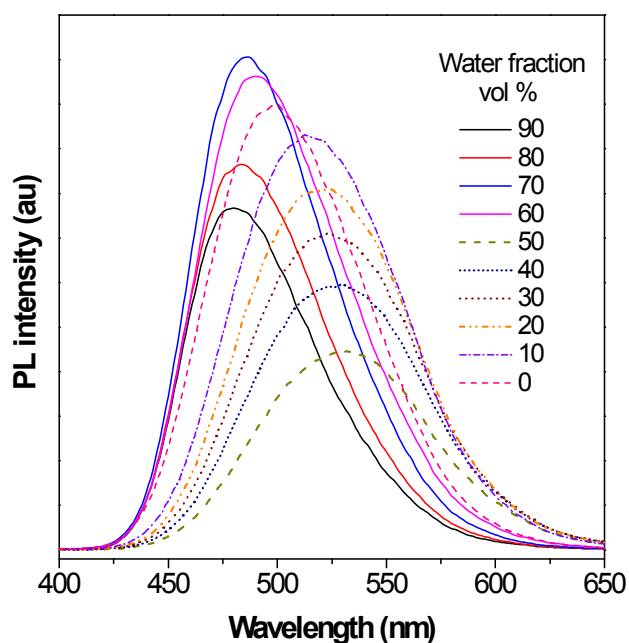


Figure S23. PL spectra of TPP-2TPA in THF/water mixtures with different water fractions; $\lambda_{\text{ex}} = 371 \text{ nm}$, $[\text{TPP-2TPA}] = 10^{-5} \text{ M}$.

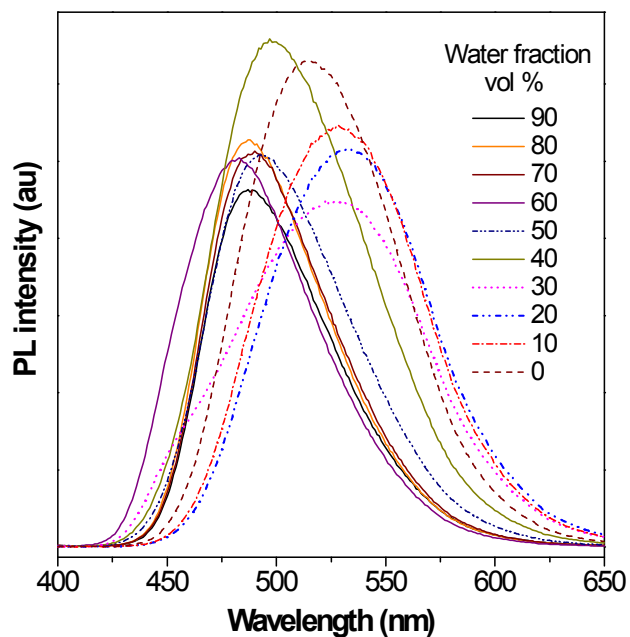


Figure S24. PL spectra of TPP-4TPA in THF-water mixtures with different water fractions; $\lambda_{\text{ex}} = 387 \text{ nm}$, $[\text{TPP-4TPA}] = 10^{-5} \text{ M}$.

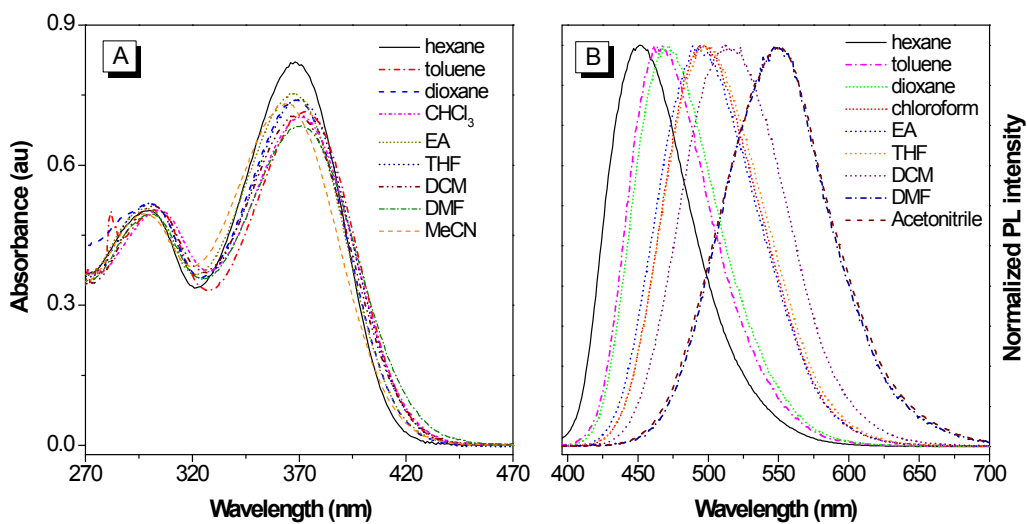


Figure S25. UV-vis spectra (A) and PL spectra (B) of TPP-2TPA in various solvents.

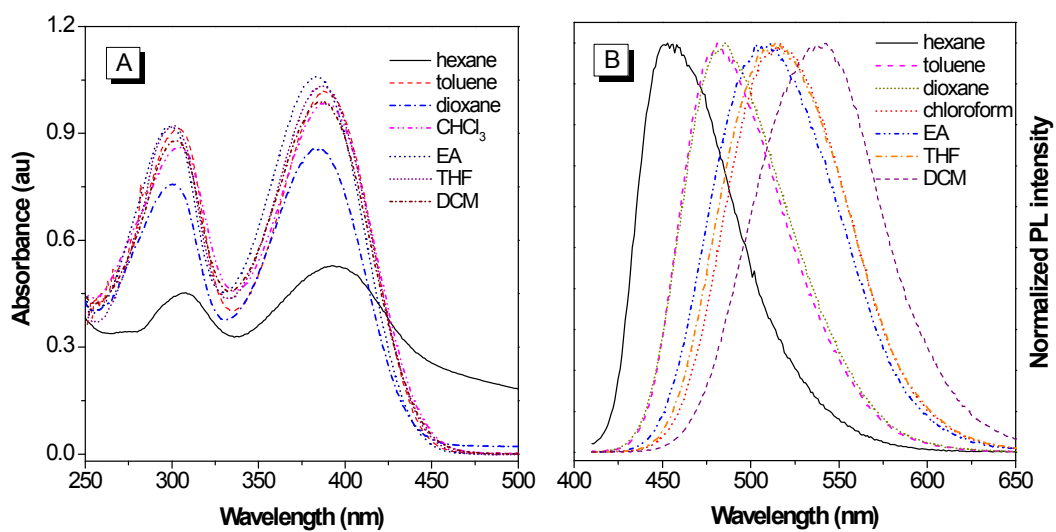


Figure S26. UV-vis spectra (A) and PL spectra (B) of TPP-4TPA in various solvent.

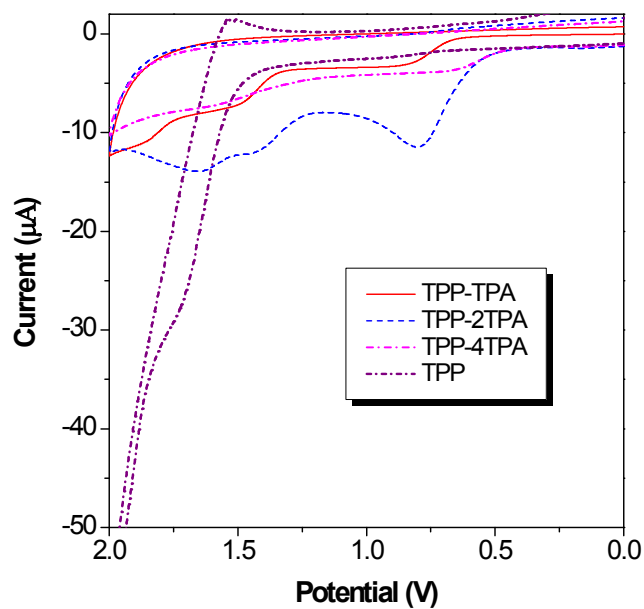


Figure S27. CV curves of TPP-TPA, TPP-2TPA, TPP-4TPA and TPP.

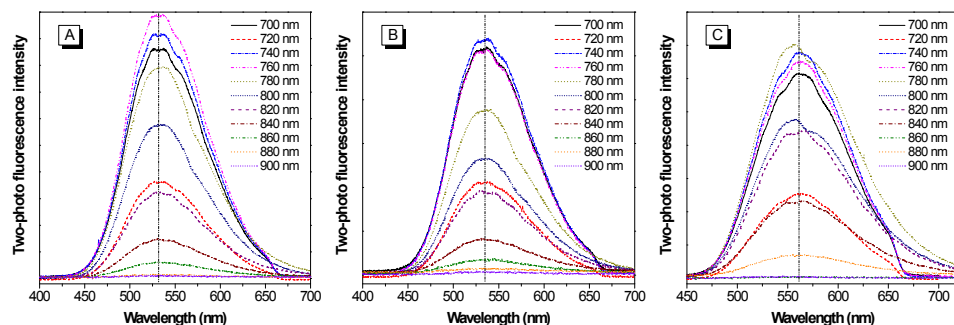


Figure S28. Two-photon PL spectra of TPP-TPA (A), TPP-2TPA (B) and TPP-4TPA (C) with various excitation wavelength in DCM.

Table S1. Optical and thermal properties of TPP derivatives.

	λ_{ab}/nm	$\lambda_{em, sol}/\text{nm}$	$\lambda_{em, solid}/\text{nm}$	$\lambda_{em, film}/\text{nm}$	$\Phi_F/\%$ ^a	$T_d/\text{°C}$
TPP-TPA	363	498	455	479	35.2	402
TPP-2TPA	371	500	481	483	16.5	504
TPP-4TPA	387	514	475	473	12.4	171,500

^a Measured using Hamamatsu Quantaurus-QY C11347 spectrometer.

Table S2. Theoretical calculation and EC properties of TPA-decorated TPP derivatives and TPP.

	E_{HOMO} ^a /eV	E_{LUMO} ^a /eV	$E_{g, calc}$ ^a /eV	E_{HOMO} ^b /eV	E_{LUMO} ^c /eV	$E_{g, opt}$ ^d /eV
TPP-TPA	-4.93	-1.51	3.42	-5.04	-2.03	3.01
TPP- 2TPA	-4.88	-1.63	3.25	-4.95	-1.99	2.96
TPP- 4TPA	-4.71	-1.51	3.20	-4.85	-2.04	2.81
TPP				-5.90	-2.58	3.32

^a Calculated by DFT/B3LYP/6-31G(d). ^b Determined by CV measurement and calculated using ferrocene HOMO level: $E_{HOMO} = -(E_{ox\ onset} - E(1/2) Fc/Fc^+ + 4.8) \text{ eV}$, $E(1/2) Fc/Fc^+ = 0.42 \text{ eV}$. ^c Calculated from the formula: $E_{HOMO} = E_{LUMO} + E_{g, opt}$. ^d Calculated from $1240/\lambda_{edge}$.

References

1. Y. Wong, K. Parthasarathy and C. Cheng, *Org. Lett.* 2010, **12**, 1736.
2. M. Chen, L. Li, H. Nie, J. Tong, L. Yan, B. Xu, J. Z. Sun, W. Tian, Z. Zhao, A. Qin and B. Z. Tang, *Chem. Sci.*, 2015, **6**, 1932.
3. (a) N. S. Makarov, M. Drobizhev and A. Rebane, *Opt. Express*, 2008, **16**, 4029; (b) X. Shen, L. Li, A. C. M. Chan, N. Gao, S. Q. Yao and Q. H. Xu, *Adv. Optical Mater.*, 2013, **1**, 92.
4. S. Cacchi, G. Fabrizi, A. Goggiamani, A. Iazzetti and R. Verdiglione, *Synthesis*, 2013, **45**, 1701.
5. H. Ren, J. Li, T. Zhang, R. Wang, Z. Gao and D. Liu, *Dyes Pigments*, 2011, **91**, 298.
6. N. S. Nandurkar, M. J. Bhanushali, M. D. Bhor and B. M. Bhanage, *Tetrahedron Lett.*, 2007, **48**, 6573.